


Research Article

Research on the Frequency Regulation Strategy of Large-Scale Battery Energy Storage in the Power Grid System

Bin He ^{1,2}, **YongFeng Ren** ^{1,2}, **Yu Xue**,^{1,2} **ChenZhi Fang**,^{1,2} **ZhiShuai Hu**,^{1,2}
and **XiaoLing Dong**³

¹College of Energy and Power Engineering, Inner Mongolia University of Technology, Hohhot 010000, China

²Key Laboratory of Wind Energy and Solar Energy Technology, Ministry of Education, Hohhot 010000, China

³School of Electrical Engineering, Southwest Jiaotong University, Chengdu 610000, China

Correspondence should be addressed to YongFeng Ren; renyongfeng@imut.edu.cn

Received 30 March 2022; Revised 4 October 2022; Accepted 17 November 2022; Published 7 December 2022

Academic Editor: Mouloud Denai

Copyright © 2022 Bin He et al. This is an open access article distributed under the Creative Commons Attribution License, which permits unrestricted use, distribution, and reproduction in any medium, provided the original work is properly cited.

Driven by the carbon peaking and carbon neutrality target, the large-scale grid-connected of renewable energy such as wind and solar has increased, and the volatility and randomness have posed new challenges to the stability of the power grid frequency. In this case, battery energy storage is a grid auxiliary resource with fast response and adjustable parameters, which can provide frequency support for the grid system in a short period. This paper studies the frequency regulation strategy of large-scale battery energy storage in the power grid system from the perspectives of battery energy storage, battery energy storage station, and battery energy storage system, respectively. First of all, the droop control based on logistic function and the virtual inertia control based on piecewise function are proposed for battery energy storage frequency regulation, which improves the performance of battery energy storage power output effectively. Second, the weighting factor is set according to the current battery charge to achieve the most optimal distribution of frequency regulation power for each battery pack in the battery energy storage station. In the end, a control framework for large-scale battery energy storage systems jointly with thermal power units to participate in system frequency regulation is constructed, and the proposed frequency regulation strategy is studied and analyzed in the EPRI-36 node model. The results of the study show that the proposed battery frequency regulation control strategies can quickly respond to system frequency changes at the beginning of grid system frequency fluctuations, which improves the stability of the new power system frequency including battery energy storage. In addition, this paper also provides a certain reference for the construction of the new power system dispatching that integrates “Generation-Grid-Load-Storage” in the future.

1. Introduction

As the world is draining fossil energy such as oil and coal, the transformation of the energy consumption structure has become a global consensus. Driven by China's carbon peak and carbon neutrality target, the country's energy system has developed toward one that is clean, low-carbon, safe, and efficient, and a new power system dominated by new energy has been set up [1, 2]. However, the new energy sources connected to the grid do not have the ability to participate in grid frequency regulation, which can put the grid frequency at great risk and even cause severe power outages [3]. On August 19, 2019, for example, Hornsea offshore windfarm

suffered a massive outage due to a chain trip that caused the frequency to fall out of the normal range, which led to power outages in parts of England and Wales for up to 1.5 hours [4, 5]. To this end, it is thus clear that maintaining the frequency stability of the power grid system is the prerequisite of its normal operation.

At present, scholars at home and abroad have conducted a lot of research on the frequency response of new energy sources connected to the grid. Literature [6] proposes a comprehensive control method including rotor kinetic energy control and pitch angle control to achieve a DFIG responding to system frequency changes directly in the full wind speed range. Literature [7] proposes an optimal

strategy for wind turbine generator auxiliary frequency control using rotor kinetic energy. The optimal frequency regulation control method for wind turbine generators is implemented in the case of insufficient rotor kinetic energy by adjusting the power output curve of the wind turbine generator. Regarding photovoltaic power generation systems, a new maximum power point tracking method based on the parameters of power deviation, voltage difference, and duty cycle change is proposed for photovoltaic systems in literature [8]. This method ensures that the power output of the photovoltaic power system is stable around the maximum power point and provides stable power support.

The research results of the abovementioned authors provide a reference basis for the new energy sources' frequency regulation. Nevertheless, the forecast of wind power and photovoltaic power involves many influencing factors, which still have some errors between the forecast and the actual. Besides, new energy sources do not provide the same stable power support as conventional energy sources when encountering extreme weather conditions such as no wind and no sun. For this reason, it is necessary to have other forms of spare capacity to participate in grid frequency regulation tasks. The battery energy storage system has the advantages of a high climbing rate, fast response speed, and high control accuracy, which can make up for the lack of active power in the grid system effectively [9]. On the one hand, battery energy storage can assist conventional units to maintain the frequency stability of the grid system; otherwise, battery energy storage can also be used as a separate frequency regulation power source to compensate for the frequency fluctuations caused by new energy grid connection [10, 11].

Meanwhile, research on energy storage participating in system frequency regulation has been carried out. In literature [12], the rule-based fuzzy logic controller of the battery energy storage is proposed for coordinated frequency and voltage support. The method was tested on the IEEE 33-node distribution network and the results showed that the battery energy storage could provide both frequency and voltage regulation support to meet the operating limits. Literature [13] proposes a coordinated frequency control strategy with rotor kinetic energy and supercapacitor energy storage, which uses rotor kinetic energy and supercapacitor to achieve inertial and droop characteristics similar to synchronous machines respectively, and ensures that the doubly-fed turbine provides a durable output when the system frequency fluctuates. Literature [14] investigated the performance of battery energy storage participating in the frequency regulation of the all-island Irish transmission system, and the results showed that sufficient capacity of battery energy storage can reduce grid frequency fluctuations effectively. The fuzzy theory approach was used to study the frequency regulation strategy of battery energy storage in the literature [15], and an economic efficiency model for frequency regulation of battery energy storage was also established. Literature [16] proposes a method for fast frequency regulation of battery based on the

amplitude phase-locked loop. Moreover, the method designs the battery to participate in primary frequency regulation and inertia emulating control based on the grid frequency deviation and differential signals detected by the amplitude phase-locked loop so that the battery can obtain better dynamic support performance. In literature [17], the frequency regulation model of a large-scale interconnected power system including battery energy storage, and flywheel energy storage system was studied. The effect of communication delay on frequency regulation control and the battery is analyzed by building a detailed model of the battery energy storage system.

In the abovementioned literature, the method of energy storage participating in frequency regulation has been studied only from a single perspective and factors such as battery charge and frequency drop deviation have not been considered. Also, there is also no in-depth study on the issue of battery pack power distribution in the full charge range and the cooperation between battery energy storage and conventional units. Hence, it is difficult to reasonably assess the advantages and disadvantages of battery energy storage participating in system frequency regulation. For this reason, this paper studies the frequency regulation control strategy concerning the large-scale BESS jointly with the thermal power units from aspects of the battery energy storage, the battery energy storage station, and the battery energy storage system, respectively. In addition, the research results also provide an approach for the dispatching control of the power grid system and also lay a theoretical foundation for the subsequent construction of a new "Generation-Grid-Load-Storage" power system.

The contribution of this paper is summarized as follows: (1) Two conventional frequency regulation methods are improved according to the battery charge, and the energy storage system can select the frequency regulation control strategy adaptively according to the system frequency drop deviation. (2) The method of battery pack distribution based on weight factor is proposed to achieve the optimal distribution of battery pack output power in the full charge range. (3) The frequency regulation control framework for battery energy storage combined with thermal power units is constructed to improve the frequency response of new power systems including energy storage systems.

The remainder of this paper is organized as follows. Chapter 2 describes the control method and strategy of battery energy storage frequency regulation and establishes two models of improved droop control and improved virtual inertia control with the feedback of battery SOC. Chapter 3 studies the power optimal distribution control strategy of each battery pack participating in the system frequency regulation from the battery energy storage station level. In Chapter 4, the frequency regulation control framework of battery energy storage-thermal power coordinated participation system is constructed. Chapter 5 verifies the capability of the battery energy storage-thermal power coordinated frequency regulation strategy through the EPRI-36 node model. Chapter 6 concludes this paper.

2. Battery Energy Storage Frequency Regulation Control Strategy

The battery energy storage system offers fast response speed and flexible adjustment, which can realize accurate control at any power point within the rated power. To this end, the lithium iron phosphate battery which is widely used in engineering is studied in this paper.

At present, the battery energy storage responds to frequency mainly by simulating the droop characteristics and inertia characteristics of the synchronous generator unit. The output power of the battery energy storage is adjusted according to the system frequency deviation to keep the system frequency stable [18]. Considering that the power output of the energy storage system is closely related to the battery SOC, using a larger charge-discharge coefficient will not only send the SOC over the limit but also shorten the life of the battery; yet, a smaller charge-discharge coefficient will be a drag on the output and make it hard to stabilize output power. Therefore, the droop control and virtual inertia control are improved based on battery SOC in this paper. Also, the improved strategy can maintain stable battery power output and reduce the damage to battery life from overcharge and overdischarge.

2.1. Improved Droop Control Strategy Based on Logistic Function. Droop control is one of the classical strategies for battery energy storage to participate in the frequency regulation of the power grid. The battery energy storage outputs active power through the droop control link, which can be expressed as follows [19]:

$$\Delta P_d = -K_d * \Delta f, \quad (1)$$

where K_d is the droop control coefficient; Δf is the frequency deviation of the power grid; ΔP_d is the increment of active power when the droop control strategy is applied to the battery energy storage.

The droop control with a fixed coefficient proves effective in frequency regulation when the system suffers a short-time load disturbance or when the SOC is sufficient. However, if such load disturbance lasts for a long time, fast charging and discharging will not only affect the working life of the battery but also send the frequency downward due to insufficient energy storage output.

In view of the above problems, this paper proposes a dynamic SOC droop control strategy for battery energy storage based on logistic function. The active power output of the battery is further adjusted by modifying the droop coefficient by the battery SOC feedback. The control block diagram is shown in Figure 1.

While preventing the overcharge and overdischarge of the battery energy storage, this strategy reduces the impact on the system when the battery energy storage exceeds the limit. In Figure 1 logistic function, the solid and dashed lines represent the discharge and charging conditions of the battery energy storage, respectively. Taking the discharge of the battery energy storage as an example, the discharge curve takes up a downward spiral. With the sufficient charge of the

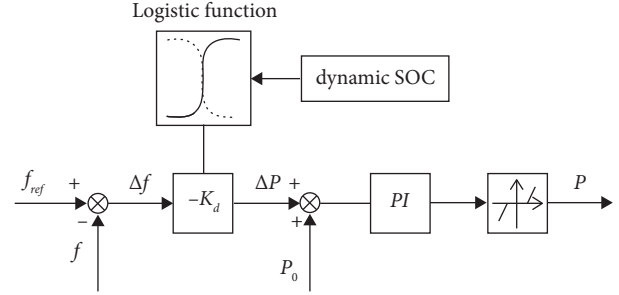


FIGURE 1: Improved droop control based on logistic function.

battery energy storage, the droop coefficient remains large, ensuring the rapid output of the battery energy storage; as the charge of the battery energy storage declines, the droop coefficient also decreases, and the discharge slows down. In that case, the charge is stabilized, which avoids over-discharge of the battery energy storage. The expression for the logistic function is as follows [20].

$$P(t) = \frac{KP_0e^{\nu t}}{K + P_0(e^{\nu t} - 1)}, \quad (2)$$

where P_0 is the initial value, the larger the P_0 , the shorter the saturation time; K is the final value; ν is an index that is used to measure the speed of curve change, the greater the value of ν , the faster the growth. Through calculation, it is most suitable to take P_0 as 0.02 and ν as 10 in this paper. Taking S_{SOC} as an independent variable, and P_0 and ν as parameter variables, the expressions of the improved droop coefficient based on the logistic function are as follows [20]:

Battery discharging:

$$K_{dd} = \frac{K_{\max}P_0e^{\nu(S_{soc}-S_{\min})/(S_{\text{high}}-S_{\min})}}{K_{\max} + P_0(e^{\nu(S_{soc}-S_{\min})/(S_{\text{high}}-S_{\min})} - 1)}. \quad (3)$$

Battery charging:

$$K_{dc} = \frac{K_{\max}P_0e^{\nu(S_{\max}-S_{soc})/(S_{\max}-S_{\text{low}})}}{K_{\max} + P_0(e^{\nu(S_{\max}-S_{soc})/(S_{\max}-S_{\text{low}})} - 1)}. \quad (4)$$

where K_{dd} and K_{dc} are the improved droop control coefficients for battery discharging and charging, respectively; K_{\max} is the final value of the improved droop coefficient; S_{SOC} is the current battery state of charge; S_{\max} is the maximum value of charge; S_{\min} is the minimum value of charge; S_{high} is the higher value of charge; S_{low} is the lower value of charge, which are 0.9, 0.1, 0.55, 0.45, respectively [21].

2.2. Improved Virtual Inertial Control Strategy Based on Piecewise Function. Battery energy storage can prevent the frequency from deteriorating by simulating the inherent inertial response process of the synchronous machine when the system frequency rises or falls seriously. The expression of virtual inertia control is as follows [22]:

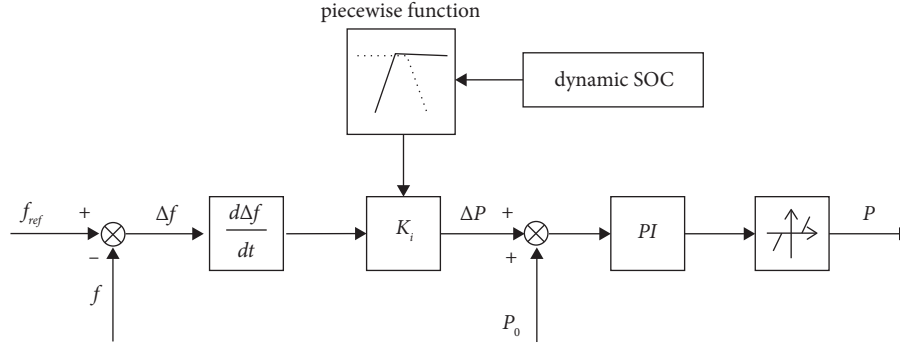


FIGURE 2: Improved virtual inertial control based on piecewise function.

$$\Delta P_i = -K_i * \frac{d\Delta f}{dt}, \quad (5)$$

where K_i is the virtual inertia control coefficient; $d\Delta f/dt$ is the frequency change rate of the power grid; ΔP_i is the active power increment when the virtual inertia strategy is used for the battery energy storage.

Considering the need for stable output from battery energy storage in the sharp slump of frequency, an improved virtual inertial control strategy based on the SOC piecewise function is proposed in this chapter. The power output of the battery energy storage is adjusted in time by modifying the virtual inertia coefficient in this method, and the control block diagram is shown in Figure 2.

As shown in the piecewise function in Figure 2, the solid line and the dotted line represent the discharge and charge operation of the battery energy storage, respectively. Taking the discharge of the battery energy storage as an example, when the battery has high capacity, the virtual inertia control coefficient adopts the maximum power coefficient for output to ensure that the battery provides stable power. When the battery capacity decreases to the inflection point, the output of the battery gradually decreases to prevent the battery from over-discharge. The expression of improved virtual inertia coefficient based on piecewise function is as follows [23]:

Battery discharging:

$$K_{id} = \begin{cases} 0, & S_{soc} \in [0, 0.1], \\ \frac{(S_{soc} - S_{min})K_{i\max}}{0.35}, & S_{soc} \in [0.1, 0.45], \\ K_{i\max}, & S_{soc} \in [0.45, 1]. \end{cases} \quad (6)$$

Battery charging:

$$K_{ic} = \begin{cases} K_{i\max}, & S_{soc} \in [0, 0.55], \\ \frac{(S_{\max} - S_{soc})K_{i\max}}{0.35}, & S_{soc} \in [0.55, 0.9], \\ 0, & S_{soc} \in [0.9, 1.0], \end{cases} \quad (7)$$

where K_{id} and K_{ic} are the improved virtual inertia control coefficients in the process of battery discharging and charging, respectively; $K_{i\max}$ is the maximum value of improved virtual inertia coefficient of battery; S_{SOC} is the current state of charge of the battery; S_{\max} and S_{\min} are the maximum and minimum values of the battery state of charge, and the value refers to Chapter 2.1.

The virtual inertial control can contain the system frequency deterioration effectively. However, the output of the battery energy storage goes against the demand for frequency restoration of the system when the frequency starts to restore. Moreover, the virtual inertial control will be a stumbling block, which is more likely to cause a secondary drop in the frequency. Therefore, it is necessary to switch to virtual negative inertia control when the frequency is recovered. By doing so, the system frequency could be recovered soon, which is in line with the requirements for the system frequency regulation.

2.3. Battery Energy Storage Integrated Control Strategy.

With a deviation in the system frequency, the droop control can effectively reduce the deviation of the system frequency and avoid the malfunction or overaction arising from the virtual inertial control to stabilize the output of the BESS. When the system frequency changes tend to be volatile, the virtual inertial control can better prevent the further deterioration of the system frequency and give play to the BESS's fast response and accurate tracking to eliminate the impact of frequency deterioration. Considering the frequency regulation effect of the battery energy storage and the characteristics and advantages of the two control methods, the improved droop control based on the logistic function is adopted in the case of small frequency deviation; the virtual inertial control based on the piecewise function is put into use when the frequency changes severely. The integrated control block diagram is shown in Figure 3.

We take the power released by the battery energy storage as an example:

- (1) The system reference frequency f is set to 50 Hz; Δf is grid frequency deviation; the dead partition range of system frequency regulation is $|\Delta f| \leq 0.033$ Hz, that is, when the system frequency is within ± 0.033 Hz, the BESS does not participate in frequency regulation [24].

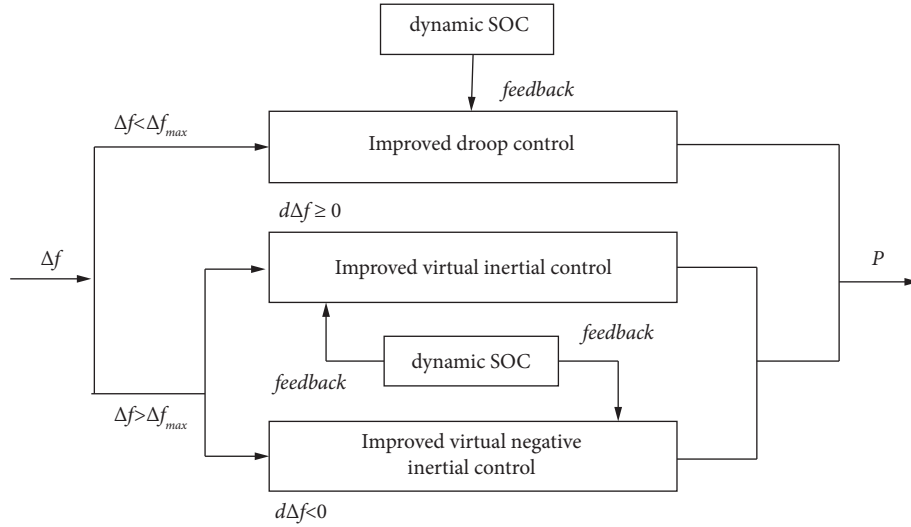


FIGURE 3: Integrated control strategy.

- (2) If the system frequency fluctuation beyond the dead partition, it is necessary to judge the battery SOC. When the charge $S_{SOC} \in [S_{min}, S_{max}]$, the energy storage system is prepared to output power. Otherwise, it will not work. When $\Delta f > 0.033$ Hz, the system load decreases and the battery is charged. On the contrary, when $\Delta f < 0.033$ Hz, the system load increases and the battery is discharged.
- (3) When the frequency deviation Δf gradually increases but does not exceed Δf_{max} , the battery energy storage uses the improved droop control in chapter 2.1 to output until the system frequency returns to normal, where the Δf_{max} is the maximum value of frequency deviation, that is, the critical switching value of virtual inertia control and droop control.
- (4) When the frequency deviation Δf gradually exceeds Δf_{max} , the improved virtual inertial control based on the piecewise function in chapter 2.2 is adopted by the BESS, and the appropriate inertial control coefficient is selected according to the size of df . When $df > 0$, the system adopts the virtual positive inertia coefficient, otherwise, it adopts the virtual negative inertia coefficient.

3. Battery Energy Storage Station Frequency Regulation Strategy

The large-scale energy storage power station is composed of thousands of single batteries in series and parallel, and the power distribution of each battery pack is the key to the coordinated control of the entire station. That makes it sensible to reasonably distribute the frequency regulation power undertaken by each battery pack in the station, allowing full play to each battery pack's frequency regulation capability.

3.1. Battery Energy Storage Pack Power Optimal Distribution Strategy. The basic battery unit in the battery energy storage station is a single lithium iron phosphate battery [25]. The battery module can be formed by connecting several single cells in series and then in parallel; the battery cluster is composed of battery modules in series; the MW-level battery energy storage pack is composed of several battery clusters connected in parallel; finally, the battery energy storage pack, power conversion system (PCS) and battery management system (BMS) are combined to form the battery energy storage station.

The distribution of active power is the core control link of the battery energy storage station. The charge of each battery energy storage pack in the battery energy storage station is different, which leads to a certain difference in the output of the battery energy storage. If the BMS is set for each battery energy storage module one by one, it will burden the communication transmission between the battery module and the battery energy storage station and seriously affect the ability of the battery energy storage to participate in the system frequency regulation.

In this case, MW-level battery pack charges are monitored in this article. The active power of each battery pack in the battery energy storage stations is distributed reasonably according to the real-time charge of the battery pack. Then, the frequency regulation control of each battery pack is carried out to achieve efficient utilization and effective output of active power. First, the charge of the battery pack is feedback to the battery energy storage station control center by the BMS; next, the battery energy storage station control center optimizes the battery packs in groups and formulates a reasonable power distribution strategy; and then sends the control command to each battery pack; finally, the battery pack adopts the corresponding control strategy to output active power according to the control command. The block diagram of the power distribution strategy in the battery energy storage power station is shown in Figure 4.

Based on the fixed coefficient active power distribution, this chapter adopts the coordinated control strategy of the battery pack with weight factor, and the frequency modulation power reference value of each battery pack can be calculated by this method. Taking the battery energy storage discharge as an example, the charge amount grouping and weight factor value of the battery pack are listed in Table 1:

The battery energy storage pack is divided into 4 groups for control according to the state of charge, and the weight factor of the battery pack with a high charge is larger than that of the battery pack with a low charge. This distribution method can give full play to the frequency modulation ability of each battery pack and realize the optimal distribution of frequency modulation power of each battery pack in the energy storage power station. The distribution factor of each battery pack can be calculated according to the weight factor and the number of battery packs [26]:

$$\lambda_{\text{BESS}} = \frac{\mu_k N_k}{\sum \mu_k N_k}, k = 1, 2, 3, \dots, \quad (8)$$

where λ_{BESS} is the distribution factor of each battery pack; μ_k is the weight factor of the charge of each battery pack; N_k is number of the battery packs with different charges.

The active power of each battery energy storage pack can be calculated by the active power demand and distribution factor of the battery energy storage station:

$$\Delta P_{\text{BP}} = \Delta P_{\text{BESS}} \lambda_{\text{BESS}}, \quad (9)$$

where ΔP_{BP} is the frequency regulation power of any battery pack in the battery energy storage station; ΔP_{BESS} is the frequency regulation power reference value of the battery energy storage station participating in the system.

3.2. Feasibility Verification of Battery Energy Storage Frequency Regulation. In the same way that conventional thermal power units function in the primary and secondary frequency regulation of the power grid system, the BESS directly adjusts the power output of each battery pack after receiving the grid frequency deviation signal in primary frequency regulation; in the case of secondary frequency regulation, similarly, it adjusts the power output through the instructions issued by the dispatching department. The control objects in the above two cases are the same, adjusting the power and capacity control system of the battery pack to stabilize the system frequency. When the system frequency drops, the BESS releases the stored energy to the grid, supplementing the active power while promoting the system frequency; when the system frequency rises, the BESS absorbs electrical energy power from the grid, consuming the active power of the grid to reduce the system frequency.

The effectiveness and feasibility of battery energy storage participating in system frequency regulation are verified in the case of the power grid load increases. The research object of battery energy storage joint with thermal power unit is verified in MATLAB/Simulink simulation software. More specifically, the simulation model includes fluctuating AC load, two thermal power synchronous units G with a capacity of 200 MW and one BESS. The BESS is a 20 MW/

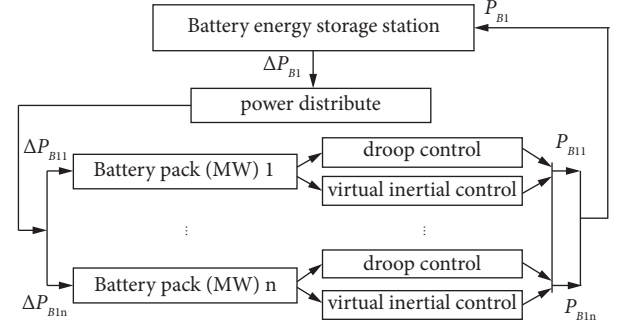


FIGURE 4: The block diagram of power distribution strategy in the energy storage power station.

TABLE 1: Charge grouping of battery pack.

Battery pack number	Charge range	Weight factor
1	[10, 30)	2
2	[30, 50)	5
3	[50, 70)	8
4	[70, 90]	10

2.5 MWh lithium iron phosphate battery pack, which has the same frequency regulation capability as a 200 MW thermal power unit [27]. The simulation model is shown in Figure 5.

On the premise that the load increases by 15 MW, the influence of the power shortage on the system frequency and the frequency regulation ability of the battery energy storage to cope with the system frequency fluctuation are studied. The fluctuation of the system frequency after the BESS is incorporated is shown in Figure 6.

From Figure 6, after the BESS is integrated into the grid, the frequency stability drops rapidly under load disturbance. The speed and amplitude of system frequency drop are significantly accelerated, which is greater than the frequency drop value before the BESS is connected to the grid. Since the battery energy storage does not participate in the system frequency regulation directly, the task of frequency regulation of conventional thermal power units is aggravated, which weakens the ability of system frequency regulation. With the gradual increase of energy storage equipment in the power grid, the situation of system frequency drop will become more and more serious.

In this case, energy storage equipment integrated into the grid also needs to play the role of assisting conventional thermal power units to participate in the system frequency regulation. Hence, the battery energy storage system cooperates with the thermal power unit to participate in the system frequency regulation strategy proposed in this paper. To verify the effectiveness and feasibility of battery energy storage participating in the system frequency regulation strategy proposed in this paper, the load increase is still 15 MW, and the system frequency changes are as shown in Figure 7.

From Figure 7, due to the characteristics of large rotational inertia and slow response speed, the conventional thermal power unit regulation system frequency is usually

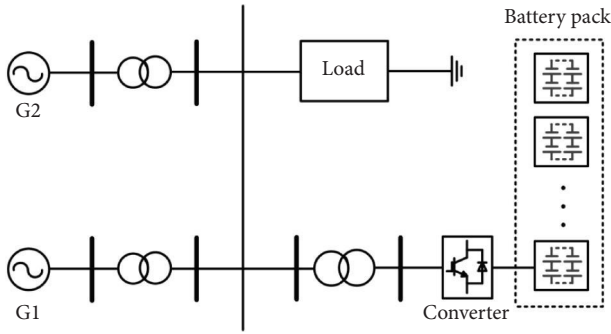


FIGURE 5: Battery energy storage system simulation.

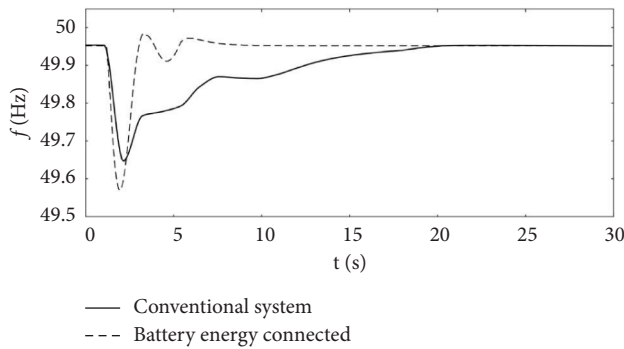


FIGURE 6: Frequency change of battery energy storage incorporated into the system.

completed in about 15 seconds. The system frequency can quickly return to stability in about 5 seconds when the BESS assists the thermal power unit to participate in the system frequency regulation, which effectively compensates for the slow response of the thermal power unit at the beginning of load fluctuations. In addition, the frequency regulation effect of the improved droop control and the improved virtual inertia control is roughly the same, but there is a certain difference in the frequency drop value. The frequency drop value of the improved droop control is 49.723 Hz, and the frequency drop value of the improved virtual inertia control is 49.741 Hz. Both control methods can provide stable active power output in the early stage of the frequency drop. Therefore, the BESS participates in the frequency regulation of the system through the frequency regulation strategy, which is more conducive to the frequency response of the system, and further shows that it is feasible for the BESS to cooperate with the thermal power unit to jointly adjust the system frequency.

4. Battery Energy Storage Thermal Power-Coordinated Frequency Regulation Strategy

The grid frequency is related to the rotational speed of conventional thermal power units in some way. In case of power shortage and frequency fluctuation in the power grid, the conventional thermal power units usually respond to system frequency changes within 5 seconds and gradually increase active power within 10 to 15 seconds, due to their

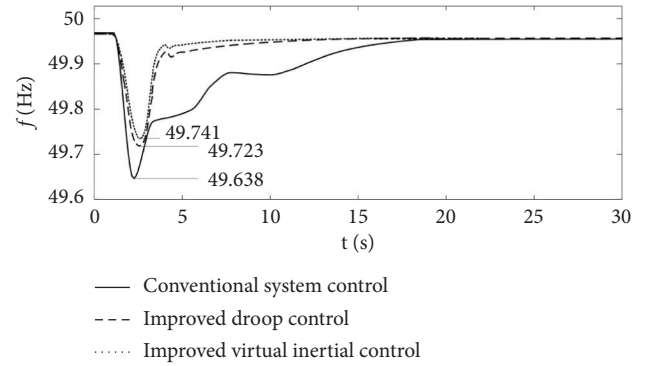


FIGURE 7: Battery energy storage participates in system frequency regulation.

characteristics such as large rotational inertia and slow response speed; until the frequency returns to stability. According to the feasibility study results of the BESS in power grid system frequency regulation as stated in chapter 3.2, with a frequency fluctuation in the system, the BESS can respond within five seconds and effectively suppress the frequency drop in most cases. To this end, to solve the problem that thermal units cannot respond to the system frequency in the first 5 seconds, the battery energy storage system cooperates with thermal units to participate in the system frequency regulation proposed in this paper. The battery energy storage system is used to compensate for the power shortage of thermal units in the first 5 seconds to achieve the purpose of regulating the frequency stability of the grid system. The framework of the battery energy storage system in cooperation with the thermal power units to participate in the system frequency regulation strategy is shown in Figure 8.

The dispatching center distributes the power shortage to the battery energy storage station control center and the thermal power plant center to realize coordinated operation through the security constraints of the power grid. This process includes the coordination of battery energy storage and thermal power units, the coordination of each battery energy storage station in the battery energy storage control center, and the coordination of each battery pack in each battery energy storage station. Specifically, when the power shortage ΔP is appeared in the power grid system, resulting in a frequency drop. The dispatching center distributes the power shortage to the thermal power plant center ΔP_G and the battery energy storage station control center ΔP_B according to the standby power uploaded in real-time by the thermal power plant center and the battery energy storage station control center. The thermal power plant center and battery energy storage station control center compensates for the power according to the power shortage distributed by the dispatching center, and feedback the additional power information P_G and P_B to the dispatching center respectively. Among them, after receiving the power shortage ΔP_B distributed by the dispatching center, the battery energy storage station control center will distribute the power shortage to each battery energy storage station $\Delta P_{B1} \dots \Delta P_{Bm}$ one by one according to the standby power uploaded in real-

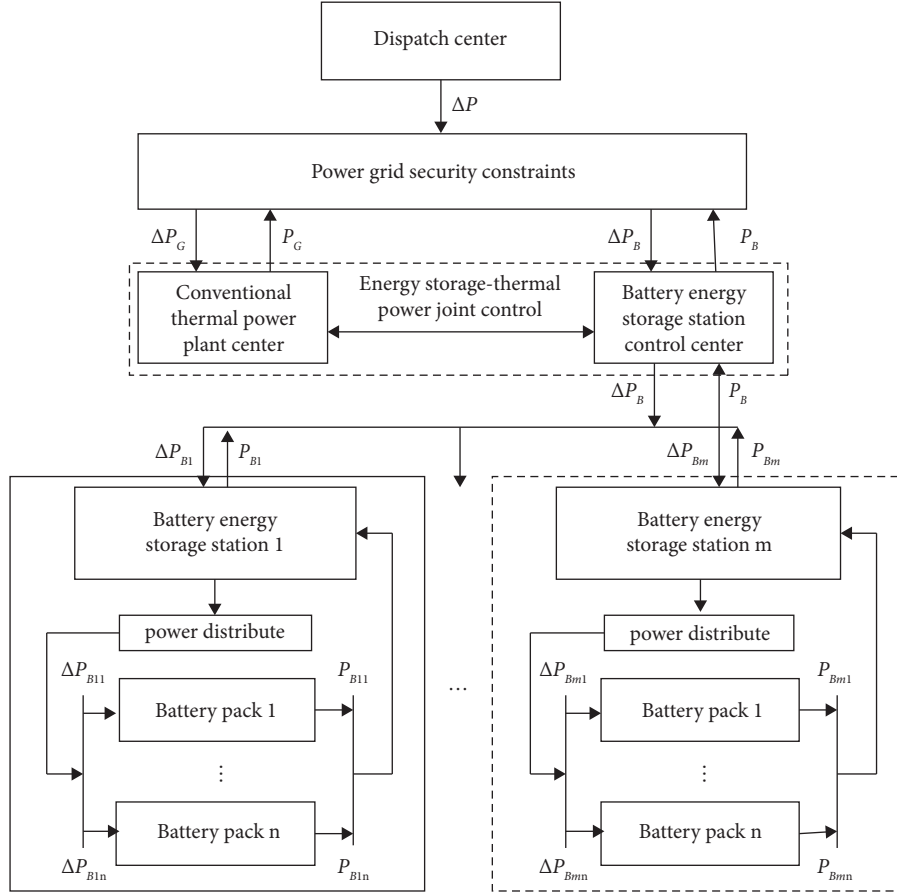


FIGURE 8: Battery energy storage-thermal power coordinated frequency regulation strategy.

time by each battery energy storage station; each battery energy storage station optimally distributes the power of each battery pack in the battery energy storage station according to the weight factor, and returns the additional power information $P_{B1} \dots P_{Bm}$ to the battery energy storage station control center one by one; after receiving the distributed power $\Delta P_{B11} \dots \Delta P_{B1n}$, each battery energy storage pack adopts the control strategy proposed in chapter 2 to provide active power, and returns the additional active power $P_{B11} \dots P_{B1n}$ to each battery energy storage station.

The total active power that can be added by the battery energy storage station is P_E ; the active power of the battery energy storage station which is distributed by the control center of the battery energy storage station is ΔP_B :

$$\Delta P_B = \begin{cases} \Delta P_B, & P_E > \Delta P_B, \\ P_E, & P_E < \Delta P_B. \end{cases} \quad (10)$$

The output power of conventional thermal power units has a hysteresis. Hence, the power of the battery energy storage station can be used for power compensation in the initial stage of system power shortage. If the power provided by the battery energy storage station is insufficient, the frequency regulation power required by the conventional thermal power unit is as follows [28]:

$$\Delta P_G = \sum_{n=1}^m P_{Gn} = \Delta P - P_E, \quad (11)$$

where P_{Gn} is the additional active power that can be generated by the n -th thermal power unit in the conventional thermal power plant; m is the number of conventional thermal power units.

5. Example Analysis

5.1. Introduction of Simulation Example. In this chapter, the EPRI-36 node model based on MATLAB/Simulink simulation software is used to study the effectiveness and feasibility of the large-scale battery energy storage coordinated thermal power frequency regulation strategy, as shown in Figure 9.

In the EPRI-36 node system, the total installed capacity of 8 conventional synchronous generator units G1~G8 and total load active power are 5112 MW and 4150 MW, respectively. Among them, the capacities of G7 and G8 are 286 MW and 388 MW, respectively. When the battery energy storage is not connected to the EPRI-36 node system, the system operates normally with an initial frequency of 49.97 Hz. The two synchronous generators G7 and G8 at the bus7 and bus8 in the system are replaced by two battery energy storage stations B1 and B2, respectively. According to the calculation, the power and capacity of the battery energy storage stations B1 and B2 with the same frequency regulation capability as the synchronous generator G7 and G8 are about 30 MW/4 MWh and 40 MW/5 MWh, respectively [27].

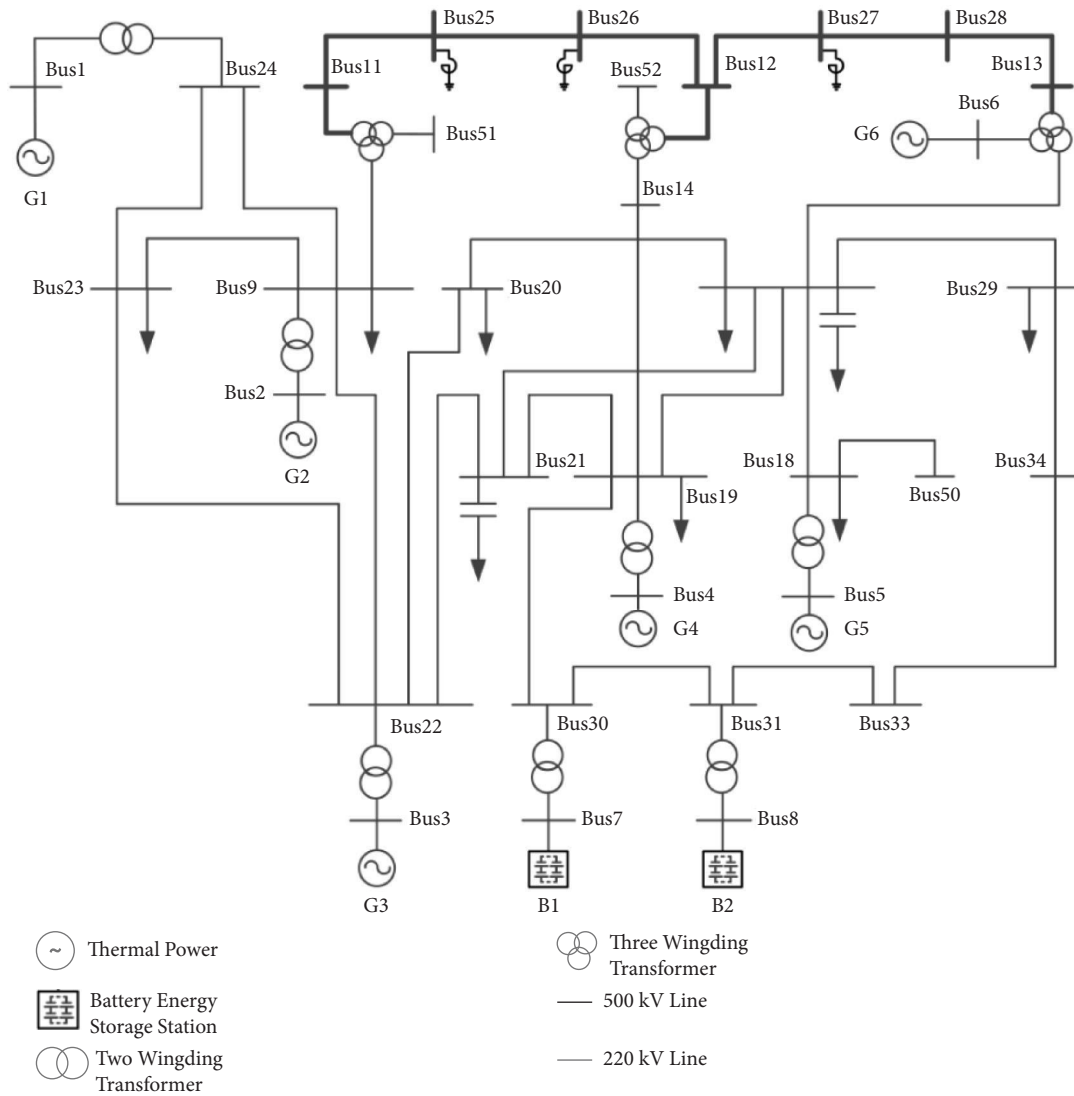


FIGURE 9: EPRI-36 node network wiring diagram including battery energy storage.

5.2. *Simulation Calculation Analysis.* The disturbance mode of the power system is load increase in this chapter, that is, 20 MW and 30 MW loads are increased at bus20 and bus33 respectively. The grid system operates normally and its initial frequency is 49.97 Hz when the BESS is not connected to the system. In addition, it is assumed that the battery energy storage has sufficient charge in the simulation process. To verify the performance of improved droop control strategy based on logistic function and improved virtual inertia control strategy based on piecewise function in a large-scale grid system, classical droop control, and virtual inertia control are added for comparative analysis in this paper. Assuming a sudden increase of 50 MW in system load at 1 second, the simulation calculation results of the improved droop control strategy are shown in Figure 10.

From Figure 10, the system frequency drops rapidly after 1 second due to a sudden increase in load. The system frequency is gradually restored to stability after 10 seconds when the conventional thermal units are generating additional active power only. The system frequency response is

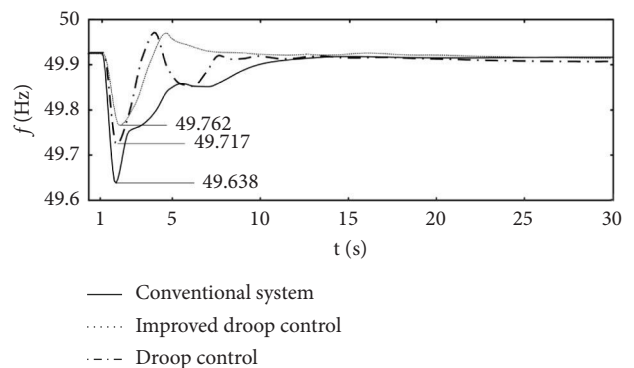


FIGURE 10: System frequency response for improved droop control.

significantly improved when the battery energy storage is added to the system to generate additional power together with the thermal power unit. In the initial stage of frequency drop, the battery energy storage quickly provides power support and thus stabilizes the system frequency in a short

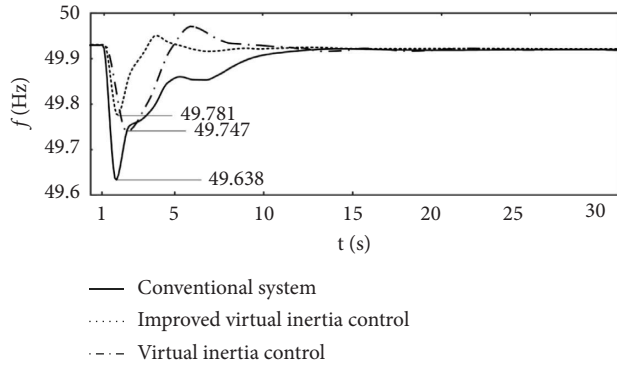


FIGURE 11: System frequency response for improved virtual inertial control.

time, which significantly shortens the restore time than the conventional thermal power units to cope with frequency fluctuation; meanwhile, the battery energy storage uses a control strategy to make the system frequency dip minimum also has a 0.124 Hz recovery. In addition, the differences between the classical droop control and the improved droop control proposed in this paper are compared in Figure 10. The system frequency was also improved after the classical droop control was adopted for the battery energy storage. However, the frequency fluctuations occurred in the process of frequency restoration, and the system frequency was restored to stability until about 8 seconds. Also, with the improved droop control strategy proposed in this paper, the system frequency is quickly restored to stability within 5 seconds. No frequency fluctuation has occurred during the restoration process. The system frequency drop value is 49.762 Hz with the improved droop control, which has a 0.045 Hz recovery from the lowest value of the classical droop control.

The simulation calculation results of the improved virtual inertia control strategy are shown in Figure 11.

From Figure 11, the drop value of system frequency is 49.747 Hz, which has a recovery of 0.109 Hz compared with the frequency drop value of conventional thermal power units, and the system frequency gradually returns to stability in about 8.5 seconds. With the improved virtual inertia control strategy proposed in the paper, the drop value of the system frequency is 49.781 Hz, which has a recovery of 0.143 Hz compared with the lowest value of the frequency drop of the conventional thermal power unit, and the system frequency returns to stability after 5.5 seconds. It can be seen that the improved virtual inertia strategy proposed in the paper is more effective in frequency regulation, which not only makes significant improvements in frequency drops but also has good results in the speed of system frequency restoration.

Combining the characteristics of slow response, stable power increase of thermal power units, and fast response of battery energy storage, this paper proposes a strategy for battery energy storage to participate in system frequency regulation together with thermal power units. The battery energy storage rapidly releases power at the early stage of frequency fluctuation; the thermal power unit steadily

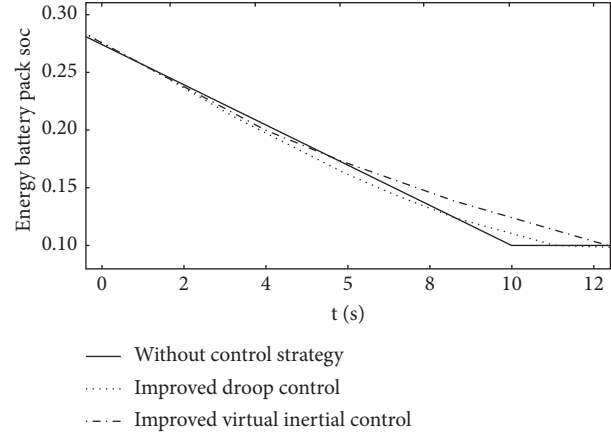


FIGURE 12: SOC of partial battery pack.

replenishes power at the middle and late stages of frequency fluctuation. The frequency response of the system was significantly improved, and stability was quickly restored within a short period. To illustrate the effectiveness of the proposed strategy in this paper, Figure 12 gives the changing states of some battery packs SOC during the power release process.

From Figure 12, the output of battery energy storage is a uniform straight line when the battery SOC is not used as feedback. The charge decreases rapidly and the battery SOC exceeds the limit, which affects the service life of the battery and may have an adverse impact on the system. The two improved control strategies proposed in this paper are to avoid overcharging and discharging the battery to a certain extent and improve the utilization of the battery. When encountering the situation of insufficient battery SOC, both control strategies can quickly adjust the output coefficient of the storage battery according to the state of charge in time to slow down the output and avoid the impact on the system caused by the battery exceeding the limit.

6. Conclusions

Aiming at the problems of low climbing rate and slow frequency response of thermal power units, this paper proposes a method and idea of using large-scale energy storage battery to respond to the frequency change of grid system and constructs a control strategy and scheme for energy storage to coordinate thermal power frequency regulation. Moreover, the simulation calculation is carried out in the EPRI-36 node arithmetic case. The conclusions are as follows:

- (1) The classical droop control and virtual inertia control are improved with battery charge as feedback. Also, the battery energy storage can respond to system frequency changes by adaptively selecting a frequency regulation strategy based on system frequency drop deviations. Compared with thermal power unit frequency regulation, the battery storage with improved droop control and improved virtual inertia control in cooperation with thermal power unit frequency regulation is enough to make the

lowest value of frequency droop have 0.124 Hz and 0.143 Hz recovery, and the system frequency can be restored to stability in about 5 s, which is shorter than the recovery time of the classical control strategy to cope with frequency fluctuations.

- (2) Aiming at the problems such as a large number of battery packs and the complicated control difficulty in the battery energy storage station, the battery pack is divided into 4 groups according to the battery charge, and the corresponding weighting factors are set, respectively, to realize the optimal distribution of the frequency regulation power of the battery pack in the battery energy storage station.
- (3) Both battery frequency regulation strategies can quickly release power at the beginning of the frequency drop, and make up for the disadvantages of slow response time and lagging frequency regulation power of thermal power units. The frequency response capability and system stability of the new power system including battery energy storage are improved effectively.

Abbreviations

BESS:	Battery energy storage station
WTG:	Wind turbine generator
PCS:	Power conversion system
BMS:	Battery management system
EPRI-36:	Electric Power Research Institute-36 Nodes System

Symbols

K_d :	Droop control coefficient
Δf :	Frequency deviation of the power grid
ΔP_d :	Output power of battery energy storage in droop control strategy
P_0 :	Initial value of logistic function
K :	Final value of logistic function
v :	Index of curve change
S_{SOC} :	Battery charge status
S_{max} :	Battery charge maximum
S_{min} :	Battery charge minimum
S_{high} :	Battery charge higher value
S_{low} :	Battery charge lower value
K_i :	Virtual inertia control coefficient
K_{imax} :	Virtual inertia coefficient maximum
K_{dd} :	Battery discharge coefficient in droop control strategy
K_{dc} :	Battery charge coefficient in droop control strategy
K_{max} :	Final value of improved droop coefficient
$d\Delta f/dt$:	Frequency change rate of the power grid
dt :	
ΔP_i :	Output power of battery energy storage in virtual inertia strategy
K_{id} :	Battery discharge coefficient in virtual inertia strategy
K_{ic} :	Battery charge coefficient in virtual inertia strategy
λ_{BESS} :	Distribution factor of each battery pack
μ_k :	Weight factor of the charge of each battery pack

N_k :	Number of the battery packs
ΔP_{BP} :	Frequency regulation power of battery pack in BESS
ΔP_{BESS} :	Reference value of frequency regulation power in BESS
P_E :	Output power provided by the BESS
ΔP_B :	Active power allocated by the control center of the BESS
P_{Gn} :	Additional active power generated by the n -th thermal power unit
m :	Number of conventional thermal power units.

Appendix

- (1) Classic droop control, virtual inertia control coefficient:

Power loop droop coefficient: $D_p = 1.4$; Power loop damping coefficient, inertia coefficient: $D = 1200$, $J = 10$; reactive power control proportional coefficient, integral coefficient: $K_p = 0.5$, $K_i = 5.0$; phase-locked loop proportion, integration coefficient: $K_p = 1.5$, $K_i = 20$; voltage outer loop proportion, integration coefficient: $K_p = 7.0$, $K_i = 2$; current inner loop proportion, integration coefficient: $K_p = 0.1$, $K_i = 10$.

- (2) G1-G6 in the 36 nodes are all conventional synchronous units, and their parameters are as follows:

G1: $S_N = 18.8$ MVA, $P_N = 15$ MW, $X_d = 0.282$ (Pu), $X_q = 0.282$ (Pu), $X_1 = 0.282$ (pu), $X'_d = 0.282$ (Pu), $X''_d = 0.282$ (Pu), $X''_q = 0.282$ (Pu), $T'_d = 10$ (s), $T''_d = 0.1$ (s), $T_j = 7.49$ (s); G2: $S_N = 7.06$ MVA, $P_N = 6$ MW, $X_d = 2.266$ (Pu), $X_q = 2.266$ (Pu), $X_1 = 2.266$ (pu), $X'_d = 0.27$ (Pu), $X''_d = 0.168$ (Pu), $X''_q = 0.168$ (Pu), $T'_d = 8.375$ (s), $T''_d = 0.224$ (s), $T_j = 4.25$ (s); G3: $S_N = 8.82$ MVA, $P_N = 7.5$ MW, $X_d = 1.217$ (Pu), $X_q = 0.6$ (Pu), $X_1 = 1.217$ (pu), $X'_d = 0.349$ (Pu), $X''_d = 0.250$ (Pu), $X''_q = 0.250$ (Pu), $T'_d = 7.24$ (s), $T''_d = 0.1$ (s), $T_j = 9.01$ (s); G4: $S_N = 2.35$ MVA, $P_N = 2.0$ MW, $X_d = 1.81$ (Pu), $X_q = 1.81$ (Pu), $X_1 = 1.81$ (pu), $X'_d = 0.284$ (Pu), $X''_d = 0.183$ (Pu), $X''_q = 0.183$ (Pu), $T'_d = 6.2$ (s), $T''_d = 0.192$ (s), $T_j = 6.67$ (s); G5: $S_N = 6.375$ MVA, $P_N = 5.1$ MW, $X_d = 1.951$ (Pu), $X_q = 1.951$ (Pu), $X_1 = 1.951$ (pu), $X'_d = 0.306$ (Pu), $X''_d = 0.198$ (Pu), $X''_q = 0.198$ (Pu), $T'_d = 6.2$ (s), $T''_d = 0.1$ (s), $T_j = 6.15$ (s); G6: $S_N = 1.0$ MVA, $P_N = 0.001$ MW, $X_d = 1.633$ (Pu), $X_q = 1.633$ (Pu), $X_1 = 1.633$ (pu), $X'_d = 0.197$ (Pu), $X''_d = 0.148$ (Pu), $X''_q = 0.148$ (Pu), $T'_d = 6.92$ (s), $T''_d = 0.1$ (s), $T_j = 2.62$ (s);

Data Availability

Research data are not shared.

Conflicts of Interest

The authors declare that there are no conflicts of interest regarding the publication of this paper.

Acknowledgments

This work was supported by National Natural Science Foundation of China, grant/award number: (51967016), (51567020), Major Science and Technology Projects of Inner Mongolia Autonomous Region: (2019ZD027), and Grid-Friendly Wind-Solar-Storage Integrated Innovative Talent Team.

References

- [1] C. Shang, "A path to planning wide-area integrated energy," *Proceedings of the CSEE*, vol. 40, no. 13, pp. 4081–4091, 2020.
- [2] M. Zeng, Y. Q. Yang, and D. N. Liu, "Generation-grid-load-storage coordinative optimal operation mode of energy internet and key technologies," *Power System Technology*, vol. 40, no. 1, pp. 114–124, 2016.
- [3] A. K. Barik and D. C. Das, "Integrated resource planning in sustainable energy-based distributed microgrids," *Sustainable Energy Technologies and Assessments*, vol. 48, Article ID 101622, 2021.
- [4] Nationalgrideso, "Appendices to the Technical Report on the Events of 9," 2019, <https://www.nationalgrideso.com/document/152351/download>.
- [5] H. D. Sun, T. Xu, and Q. Guo, "Analysis on blackout in great britain power grid on august 9th, 2019 and its enlightenment to power grid in China," *Proceedings of the CSEE*, vol. 39, no. 21, pp. 6183–6191, 2019.
- [6] P. H. Yang, B. He, B. Wang et al., "Coordinated control of rotor kinetic energy and pitch angle for large-scale doubly fed induction generators participating in system primary frequency regulation," *IET Renewable Power Generation*, vol. 15, no. 8, pp. 1836–1847, 2021.
- [7] M. Sun, F. Xu, and L. Chen, "Optimal auxiliary frequency control strategy of wind turbine generator utilizing rotor kinetic energy," *Proceedings of the CSEE*, vol. 42, no. 2, pp. 506–513, 2021.
- [8] U. Datta, A. Kalam, and J. Shi, "Battery energy storage system control for mitigating PV penetration impact on primary frequency control and state-of-charge recovery," *IEEE Transactions on Sustainable Energy*, vol. 11, no. 2, pp. 746–757, 2020.
- [9] D. W. Su and Z. Lei, "Optimal configuration of battery energy storage system in primary frequency regulation," *Energy Reports*, vol. 7, no. 6, pp. 157–162, 2021.
- [10] U. Akram, M. Nadarajah, R. Shah, and F. Milano, "A review on rapid responsive energy storage technologies for frequency regulation in modern power systems," *Renewable and Sustainable Energy Reviews*, vol. 120, Article ID 109626, 2020.
- [11] L. X. Meng, J. Zafar, S. K. Khadem et al., "Fast frequency response from energy storage systems—A review of grid standards, Projects and technical issues," *IEEE Transactions on Smart Grid*, vol. 11, no. 2, pp. 1566–1581, 2020.
- [12] W. Liu, Y. Xu, X. Feng, and Y. Wang, "Optimal fuzzy logic control of energy storage systems for V/f support in distribution networks considering battery degradation," *International Journal of Electrical Power & Energy Systems*, vol. 139, Article ID 107867, 2022.
- [13] X. W. Yan, X. W. Sun, and S. Cui, "Improved control strategy for inertia and primary frequency regulation of doubly fed induction generator based on rotor kinetic energy and supercapacitor energy storage," *Transactions of China Electrotechnical Society*, vol. 36, pp. 179–190, 2021.
- [14] F. Arrigo, E. Bompard, M. Merlo, and F. Milano, "Assessment of primary frequency control through battery energy storage systems," *International Journal of Electrical Power & Energy Systems*, vol. 115, no. 2, Article ID 105428, 2020.
- [15] J. H. Li, Z. Gao, G. Mu, X. Fan, Z. Zhang, and J. Zou, "Research on the control strategy of energy storage participation in power system frequency regulation," *International Transactions on Electrical Energy Systems*, vol. 30, no. 12, Article ID 12676, 2020.
- [16] L. Shang, X. Z. Dong, C. X. Liu, and Z. Gong, "Fast grid frequency and voltage control of battery energy storage system based on the amplitude-phase-locked-loop," *IEEE Transactions on Smart Grid*, vol. 13, no. 2, pp. 941–953, 2022.
- [17] N. S. Guzman E, C. A. Cañizares, K. Bhattacharya, and D. Sohm, "Frequency regulation model of bulk power systems with energy storage," *IEEE Transactions on Power Systems*, vol. 37, no. 2, pp. 913–926, 2022.
- [18] M. M. Rahman, A. O. Oni, E. Gemechu, and A. Kumar, "The development of techno-economic models for the assessment of utility-scale electro-chemical battery storage systems," *Applied Energy*, vol. 283, Article ID 116343, 2021.
- [19] W. Xing, H. W. Wang, L. G. Lu, S. Wang, and M. Ouyang, "An adaptive droop control for distributed battery energy storage systems in microgrids with DAB converters," *International Journal of Electrical Power & Energy Systems*, vol. 130, Article ID 106944, 2021.
- [20] Z. X. Fu, J. J. Zhang, and X. D. Cui, "Research on optimal control strategy of photovoltaic system supported by energy storage participating in primary frequency regulation of power grid," *Renewable Energy Resources*, vol. 39, no. 11, pp. 1530–1540, 2021.
- [21] X. W. Yan and S. Cui, "Primary frequency regulation control strategy of doubly-fed induction generator considering supercapacitor SOC feedback adaptive adjustment," *Transactions of China Electrotechnical Society*, vol. 36, no. 5, pp. 1027–1039, 2021.
- [22] B. Liu, J. B. Zhao, Q. Huang, F. Milano, Y. Zhang, and W. Hu, "Nonlinear virtual inertia control of WTGs for enhancing primary frequency response and suppressing drivetrain torsional oscillations," *IEEE Transactions on Power Systems*, vol. 36, no. 5, pp. 4102–4113, 2021.
- [23] X. Deng, W. Sun, and H. W. Xiao, "Integrated control strategy of battery energy storage system in primary frequency regulation," *High Voltage Engineering*, vol. 44, no. 3, pp. 1157–1165, 2018.
- [24] Z. S. Zhu, C. T. Ye, and S. Y. Wu, "Comprehensive control method of energy storage system to participate in primary frequency regulation with adaptive state of charge recovery," *International Transactions on Electrical Energy Systems*, vol. 31, no. 12, Article ID 13220, 2021.
- [25] T. A. Vitor, N. C. R. Maria de Fátima, and C. M. Aghatta, "Laboratory studies in different battery technologies for application in transportable energy storage systems," in *Proceedings of the 2021 IEEE PES Innovative Smart Grid*

Technologies Europe, pp. 405–409, Espoo, Finland, October 2021.

- [26] X. N. Li, L. X. Lyu, G. C. Geng et al., “Power allocation strategy for battery energy storage system based on cluster switching,” *IEEE Transactions on Industrial Electronics*, vol. 69, no. 4, pp. 3700–3710, 2022.
- [27] J. L. Li, J. Y. Huang, and K. Fang, *Frequency Regulation of Electric Power System Using Battery Energy Storage System*, pp. 110–112, China Machine Press, Beijing, China, 2018.
- [28] C. M. Zhang, L. Liu, H. Z. Cheng, D. Liu, J. Zhang, and G. Li, “Frequency-constrained Co-planning of generation and energy storage with high-penetration renewable energy,” *Journal of Modern Power Systems and Clean Energy*, vol. 9, no. 4, pp. 760–775, 2021.